Nonlinear Dyn (2014) 78:2141–2159
DOI 10.1007/s11071-014-1572-1

ORIGINAL PAPER

Coupling-observer-based nonlinear control for flexible air-breathing hypersonic vehicles

Na Wang · Huai-Ning Wu · Lei Guo

Received: 21 May 2013 / Accepted: 29 June 2014 / Published online: 24 July 2014

Abstract This paper investigates the nonlinear control problem for flexible air-breathing hypersonic vehicles (FAHVs). The coupling dynamics between flexible and rigid-body parts of FAHVs may cause degradation of control performance or high-frequency oscillations of control input and flexible state. In this paper, the flexible effects produced by the coupling are modeled as a kind of unknown disturbance and included in the new control-design model, for which a coupling observer is constructed to estimate these effects. Thus, a novel nonlinear composite control strategy, which combines a coupling-observer-based feedforward compensator and a dynamic-inversion-based feedback controller, is proposed to reject the flexible effects on pitch rate and track desired trajectories of velocity and flight-path angle. The stability of composite closed-loop system is analyzed by using the Lyapunov theory. Simulation results on a full nonlinear model of FAHVs demonstrate that the presented controller is more effective by comparison with the previous scheme.

Keywords Flexible air-breathing hypersonic vehicles · Rigid-flexible coupling dynamics · Coupling observer · Disturbance observer-based control · Composite hierarchical anti-disturbance control

N. Wang
School of Instrumentation Science and Opto-Electronics Engineering, Beihang University, Xue Yuan Road No. 37, Hai Dian District, Beijing 100191, People's Republic of China

N. Wang
National Key Laboratory of Aerospace Intelligent Control Technology, Beijing Aerospace Automatic Control Institute, Beijing 100854, People's Republic of China
e-mail: wangnaflcon@126.com

H.-N. Wu
School of Automation Science and Electrical Engineering, Beihang University, Xue Yuan Road No. 37, Hai Dian District, Beijing 100191, People's Republic of China
e-mail: whn@buaa.edu.cn

L. Guo (✉)
National Key Laboratory on Aircraft Control Technology, Beihang University, Xue Yuan Road No. 37, Hai Dian District, Beijing 100191, People's Republic of China
e-mail: lguo@buaa.edu.cn

1 Introduction

Air-breathing hypersonic vehicles (AHVs) present a cost efficient way to make access to space routine. But it uses scramjet engines integrated with the airframe, so the vehicle dynamics display strong interactions between the elastic airframe and the propulsion system (see [1–3] and references therein). In addition, significant flexible effects cannot be neglected in the control design due to the slender geometries and light structures of flexible air-breathing hypersonic vehicles (FAHVs) (see [4–6] and references therein). Thus, flight control of AHVs is very important and difficult especially for FAHVs.

In the past few years, many effective modeling and control techniques have been presented for AHVs (see e.g. [6–31]). The available control methods can be divided into two subcategories: linear model based and nonlinear model based. The linear approaches are simple and easily performed, but the capability of the linear models to represent the dynamics and the coupling effects is limited (see e.g. [11–17]). As such, nonlinear models that carry more information instead of linear ones have been investigated (see e.g. [18–31]). Many nonlinear control methods were successfully applied for a model of AHVs developed at NASA Langley Research Center (see e.g. [18–28]). For example, an effective neural control method via time-scale decomposition with throttle setting constraint was proposed for this AHV model in [26]. But rigid-body dynamics were only contained in the nonlinear AHV model.

Therefore, a nonlinear model of FAHVs was developed by Bolender and Doman in [6], which includes not only the interactions between the propulsion system and the airframe dynamics, but also the strong flexible effects. Based on this nonlinear model of FAHVs, a control-design model in closed form was obtained by replacing complex force and moment functions with curve-fitted approximations in [29]. Many nonlinear controllers were applied effectively for the curve-fitted model (see e.g. [29–31]). However, the nonlinear controllers proposed in [29] and [30] were constructed based on control-design models without including the rigid-flexible coupling dynamics. It has been shown that the undesired flexible effects may cause degradation of the performance of flight control systems in [29]. So the rigid-flexible coupling dynamics should be considered and studied to design nonlinear controllers for FAHVs. In [31], the flexible effects were transformed into some terms that depended on the flexible modes and appeared in forces and moment. Since many coefficients used for approximating these effects have to be estimated by using adaptive methods, it may lead to a large amount of calculations online. To overcome these problems, the flexible effects on pitch rate produced by rigid-flexible coupling dynamics are considered as a kind of unknown disturbance and modeled using known information in this paper. Then a coupling-observer-based nonlinear controller, which is a novel nonlinear composite controller, is proposed to reject the flexible effects and track the desired trajectories.

Recently, the disturbance-observer-based control strategy has attracted considerable attention. In most cases, principle of disturbance observer design in the time domain is similar to the one of state observer presented in [32], which can be concluded as follows: with suitable selection of disturbance observer gain, the dynamics of disturbance observer must be faster than the ones of the actual system, so that the estimate of disturbance can approach the actual disturbance as quickly as possible. In [34], it has been shown that this kind of composite hierarchical anti-disturbance control scheme can be applied to solve many control problems with multiple disturbances. Moreover, it has been applied effectively in many practical systems (see e.g. [12,22,27,35]). For example, a disturbance-observer-based dynamic inversion controller was designed first for missile systems in [35], and several effective composite control methods based on disturbance observer have been presented for the AHV model in [12,22,27]. However, the study for the nonlinear FAHV model with rigid-flexible coupling dynamics using composite control strategy is still insufficient due to its special structure.

In conclusion, the main contributions in this paper can be summarized as follows:

(1) The flexible effects on pitch rate are formulated as a kind of unknown disturbance, which is considered in the control-design model and estimated by a coupling observer.
(2) Combining a dynamic-inversion-based controller with a coupling-observer-based compensator, a novel nonlinear composite controller is proposed to make velocity and flight-path angle track desired signals and reject the flexible effects.
(3) The stability of composite closed-loop system which combines two tracking-error equations and a coupling estimation error equation is analyzed.

In simulation studies, it will be demonstrated that the rigid-flexible coupling dynamics may cause degradation of control performance or high-frequency oscillations of control input and flexible state using the nonlinear controller presented in [29], while the proposed coupling-observer-based nonlinear controller can avoid these problems successfully.

The rest of the paper is organized as follows. In Sect. 2, the FAHV model is introduced and the control objective is defined. In Sect. 3, a novel nonlinear composite controller is proposed. Simulation results are given in Sect. 4. Finally, some conclusions are drawn in Sect. 5.

Notation The notations used throughout the paper are standard. The superscript "T" and "-1" stand for transpose and inversion of a matrix or vector, respectively. R^n denotes the n-dimensional Euclidean space, the notation $P > 0$ means that P is a real symmetric and positive definite matrix, I and 0 represent the identity matrix and a zero matrix, respectively. diag{...} stands for a block-diagonal matrix, $\|\cdot\|$ denotes the Euclidean norm of a vector and its induced norm of a matrix.

2 Problem formulation

A nonlinear model for the longitudinal dynamics of flexible air-breathing hypersonic vehicles (FAHVs), as given by Bolender and Doman in [6], is described by the following nonlinear equations:

$$\dot{h} = V \sin\gamma, \tag{1}$$

$$\dot{V} = \frac{T\cos\alpha - D}{m} - g\sin\gamma, \tag{2}$$

$$\dot{\alpha} = -\frac{L + T\sin\alpha}{mV} + Q + \frac{g}{V}\cos\gamma, \tag{3}$$

$$\dot{\gamma} = \frac{L + T\sin\alpha}{mV} - \frac{g}{V}\cos\gamma, \tag{4}$$

$$I_{yy}\dot{Q} = M + \tilde{\psi}_1\ddot{\eta}_1 + \tilde{\psi}_2\ddot{\eta}_2, \tag{5}$$

$$\ddot{\eta}_i = -2\zeta_i\omega_i\dot{\eta}_i - \omega_i^2\eta_i + N_i + \tilde{\psi}_i\dot{Q},\ i = 1, 2. \tag{6}$$

The model is composed of rigid-body state $x_r = [h\ V\ \alpha\ \gamma\ Q]^T$, control input $u = [\delta_e\ \Phi]^T$ and flexible modes η_1 and η_2, whereas the output to be controlled is selected as $y = [V\ \gamma]^T$. The nomenclature is given in Table 1. The fuel equivalence ratio affects the thrust directly and the pitching moment indirectly via coupling between the engine and the airframe. The aerodynamic forces/moment and the generalized elastic forces are influenced by the aerodynamic control surfaces.

Remark 1 The FAHV nonlinear model described by (1)–(6) has strong interactions among rigid-body state, control input, and flexible modes due to rigid-flexible coupling dynamics (that is, $\tilde{\psi}_1\ddot{\eta}_1 + \tilde{\psi}_2\ddot{\eta}_2$ and $\tilde{\psi}_i\dot{Q}$). It may cause the performance degradation to design nonlinear controller without considering these couplings (see [6] and [29]). The flexible effects were studied and added in the approximations of forces and moment in [31]. However, it may lead to a large amount of calculations online because many coefficients (such as C_L^η, C_D^η, C_M^η and $C_{N_i}^\eta$) have to be estimated using the adaptive methods. To avoid these problems, the flexible effects on pitch rate are modeled as a kind of unknown disturbance in this paper, which is estimated by a coupling observer. And then, a feedforward compensator based on the coupling observer is designed to reject these flexible effects.

Table 1 Nomenclature

h	Altitude
V	Velocity
α	Angle of attack
γ	Flight path angle
θ	Pitch angle, $\theta = \alpha - \gamma$
Q	Pitch rate, $Q = \dot{\theta}$
η_i	Generalized elastic coordinate
Φ	Fuel equivalence ratio
δ_e	Elevator deflection
N_i	Generalized elastic force
L	Lift
D	Drag
T	Thrust
M	Pitching moment
m	Vehicle mass
I_{yy}	Moment of inertia
g	Acceleration due to gravity
$\tilde{\psi}_i$	Inertial coupling parameter
ζ_i	Damping ratio for η_i
ω_i	Natural frequency for η_i

The approximations of the forces and moment adopted in this paper are given by Parker and Fiorentini in [29], which are described as follows:

$$L = qS(C_L^\alpha\alpha + C_L^0 + C_L^{\delta_e}\delta_e),$$

$$D = qS(C_D^{\alpha^2}\alpha^2 + C_D^\alpha\alpha + C_D^0 + C_D^{\delta_e^2}\delta_e^2 + C_D^{\delta_e}\delta_e),$$

$$T = (C_{T\Phi}^{\alpha^3}\alpha^3 + C_{T\Phi}^{\alpha^2}\alpha^2 + C_{T\Phi}^\alpha\alpha + C_{T\Phi}^0)\Phi + C_T^{\alpha^3}\alpha^3 + C_T^{\alpha^2}\alpha^2 + C_T^\alpha\alpha + C_T^0,$$

$$M = z_T T + qS\bar{c}(C_M^{\alpha^2}\alpha^2 + C_M^\alpha\alpha + C_M^0 + C_M^{\delta_e}\delta_e),$$

$$N_1 = C_{N_1}^{\alpha^2}\alpha^2 + C_{N_1}^\alpha\alpha + C_{N_1}^0,$$

$$N_2 = C_{N_2}^{\alpha^2}\alpha^2 + C_{N_2}^\alpha\alpha + C_{N_2}^0 + C_{N_2}^{\delta_e}\delta_e,$$

where $C_M^{(\cdot)}$, $C_T^{(\cdot)}$, $C_{T\Phi}^{(\cdot)}$, $C_{N_i}^{(\cdot)}$, $C_L^{(\cdot)}$, and $C_D^{(\cdot)}$ are the coefficients of the curve-fit approximations. S denotes the reference area, $\bar{c}$ the mean aerodynamic chord and z_T the thrust moment arm. Dynamic pressure $q =$

Table 2 Admissible ranges for variables

Variable	Min. value	Max. value
h	70,000 ft	135,000 ft
V	7,000 ft/s	11,000 ft/s
α	$-5°$	$10°$
γ	$-3°$	$3°$
Q	$-10°$	$10°$
q	500 psf	2000 psf
Φ	0.05	1.5
δ_e	$-20°$	$20°$

$(\rho V^2)/2$ and air density $\rho = \rho_0 \exp(-(h-h_0)/h_s)$, in which h_s^{-1} is the air density decay rate, ρ_0 and h_0 are the values of air density and altitude at trimmed cruise condition.

Similarly to [30] and [31], the hypersonic cruising regimes are only considered for the above nonlinear model in this paper. As consequence of the physical constraints that characterize hypersonic flight and operability of scramjet engines, the rigid-body state x_r is bound to remain within the admissible range shown in Table 2, which determine the flight envelope, together with the admissible range for the control input u. And the admissible ranges for variables in Table 2 are same as the ones of Table 1 in [31].

In this paper, our objective is to design a nonlinear control law such that the output y can track the desired signals $[V_d \quad \gamma_d]^T$ for the nonlinear model of FAHVs, where the desired trajectories are assumed to be bounded and with bounded derivatives of any order. The next section is to provide a novel nonlinear composite controller to achieve the control objective.

3 Coupling-observer-based nonlinear controller design

This section presents a novel composite controller with a hierarchical architecture for the nonlinear model of FAHVs. First, a control-design model with rigid-flexible coupling dynamics is provided. Second, the coupling observer is constructed to estimate the flexible effects on pitch rate. Finally, the nonlinear composite controller, which combines a coupling-observer-based compensator and a dynamic-inversion-based controller, is proposed to reject the flexible effects and track the desired trajectories. In addition, stability of the composite closed-loop system involving two tracking-error equations and a coupling observation error equation is analyzed.

3.1 Control-design model

Similarly to [29], the control-design model for rigid-body variables is obtained from the FAHV nonlinear model (1)-(6) by removing the altitude and flexible modes and setting to zero the weak elevator couplings, which is given by following equations:

$$\dot{V} = f_1(x_r, \Phi), \tag{7}$$

$$\dot{\alpha} = f_2(x_r, \Phi), \tag{8}$$

$$\dot{\gamma} = f_3(x_r, \Phi), \tag{9}$$

$$\dot{Q} = f_4(x_r, \Phi) + g_4(x_r, \Phi)\delta_e + d_c, \tag{10}$$

where nonlinear functions $f_1(x_r, \Phi)$, $f_2(x_r, \Phi)$, $f_3(x_r, \Phi)$, $f_4(x_r, \Phi)$, and $g_4(x_r, \Phi)$ are sufficiently smooth with respect to x_r and Φ, disturbance d_c is produced by the rigid-flexible coupling dynamics. The concrete forms of $f_1(x_r, \Phi)$, $f_2(x_r, \Phi)$, $f_3(x_r, \Phi)$, $f_4(x_r, \Phi)$, $g_4(x_r, \Phi)$, and d_c are described as $f_1(x_r, \Phi) = (T\cos\alpha - \bar{D})/m - g\sin\gamma$, $f_2(x_r, \Phi) = -(\bar{L} + T\sin\alpha)/(mV) + Q + (g/V)\cos\gamma$, $f_3(x_r, \Phi) = (\bar{L} + T\sin\alpha)/(mV) - (g/V)\cos\gamma$, $f_4(x_r, \Phi) = \bar{I}_{yy}^{-1}[z_T T + q S\bar{c}(C_M^{\alpha^2}\alpha^2 + C_M^{\alpha}\alpha + C_M^0) + \tilde{\psi}_1 N_1 + \tilde{\psi}_2(C_{N_2}^{\alpha^2}\alpha^2 + C_{N_2}^{\alpha}\alpha + C_{N_2}^0)]$, $g_4(x_r, \Phi) = \bar{I}_{yy}^{-1}(q S\bar{c}C_M^{\delta_e} + \tilde{\psi}_2 C_{N_2}^{\delta_e})$ and $d_c = C_f[\eta_1 \quad \eta_2 \quad \dot{\eta}_1 \quad \dot{\eta}_2]^T$, where $\bar{L} = qS(C_L^{\alpha}\alpha + C_L^0)$, $\bar{D} = qS(C_D^{\alpha^2}\alpha^2 + C_D^{\alpha}\alpha + C_D^0)$, $\bar{I}_{yy} = I_{yy} - \tilde{\psi}_1^2 - \tilde{\psi}_2^2$ and $C_f = \bar{I}_{yy}^{-1}[-\tilde{\psi}_1\omega_1^2 \quad -\tilde{\psi}_2\omega_2^2 \quad -2\tilde{\psi}_1\zeta_1\omega_1 \quad -2\tilde{\psi}_2\zeta_2\omega_2]$.

Remark 2 It is different from [29] that the flexible effects produced by the rigid-flexible coupling dynamics are considered and added in the control-design model (7)–(10).

Using (5) and (6), the model for flexible modes η_1 and η_2, which is provided to construct the coupling observer in next subsection, can be written as

$$\dot{x}_f = A_f x_f + B_f(x_r)\delta_e + F_f(x_r, \Phi), \tag{11}$$

where $x_f = [\eta_1 \quad \eta_2 \quad \dot{\eta}_1 \quad \dot{\eta}_2]^T$ is the flexible state, and

$$A_f = \begin{bmatrix} 0 & 0 & 1 & 0 \\ 0 & 0 & 0 & 1 \\ -p_1\omega_1^2 & -p_3\omega_2^2 & -2p_1\zeta_1\omega_1 & -2p_3\zeta_2\omega_2 \\ -p_3\omega_1^2 & -p_2\omega_2^2 & -2p_3\zeta_1\omega_1 & -2p_2\zeta_2\omega_2 \end{bmatrix},$$

$$B_f(x_r) = \begin{bmatrix} 0 \\ 0 \\ b_{f1} \\ b_{f2} \end{bmatrix}, \quad F_f(x_r, \Phi) = \begin{bmatrix} 0 \\ 0 \\ f_{f1} \\ f_{f2} \end{bmatrix},$$

in which $p_1 = 1 + \bar{I}_{yy}^{-1}\tilde{\psi}_1^2$, $p_2 = 1 + \bar{I}_{yy}^{-1}\tilde{\psi}_2^2$, $p_3 = \bar{I}_{yy}^{-1}\tilde{\psi}_1\tilde{\psi}_2$, $b_{f1} = \bar{I}_{yy}^{-1}\tilde{\psi}_1 q S\bar{c}C_M^{\delta_e} + p_3 C_{N_2}^{\delta_e}$, $b_{f2} = \bar{I}_{yy}^{-1}\tilde{\psi}_2 q S\bar{c}C_M^{\delta_e} + p_2 C_{N_2}^{\delta_e}$, $f_{f1} = \bar{I}_{yy}^{-1}\tilde{\psi}_1[z_T T + qS\bar{c}(C_M^{\alpha^2}\alpha^2 + C_M^{\alpha}\alpha + C_M^0)] + p_3(C_{N_2}^{\alpha^2}\alpha^2 + C_{N_2}^{\alpha}\alpha + C_{N_2}^0) + p_1 N_1$, $f_{f2} = \bar{I}_{yy}^{-1}\tilde{\psi}_2[z_T T + qS\bar{c}(C_M^{\alpha^2}\alpha^2 + C_M^{\alpha}\alpha + C_M^0)] + p_3 N_1 + p_2(C_{N_2}^{\alpha^2}\alpha^2 + C_{N_2}^{\alpha}\alpha + C_{N_2}^0)$.

3.2 Coupling observer design

We can construct a nonlinear Luenberger observer to estimate the flexible state x_f based on (10) and (11). So a coupling observer to estimate the unknown disturbance d_c can be given by

$$\begin{cases} \hat{d}_c = C_f\hat{x}_f \\ \hat{x}_f = v_c + L_c Q \\ \dot{v}_c = (A_f - L_c C_f)(v_c + L_c Q) + B_f(x_r)\delta_e \\ \qquad +F_f(x_r, \Phi) - L_c(f_4(x_r, \Phi) + g_4(x_r, \Phi)\delta_e), \end{cases} \tag{12}$$

where $\hat{d}_c$ and $\hat{x}_f$ are estimates of d_c and x_f, respectively. Besides, v_c is the internal state of observer (12) and the observer gain, $L_c \in \mathcal{R}^{4\times 1}$, is to be designed.

Define flexible state estimation error $e_f(t) = x_f - \hat{x}_f$ and coupling estimation error $e_c(t) = d_c - \hat{d}_c$. Obviously, $e_c(t) = C_f e_f(t)$. Using coupling observer (12), the first differential of $e_f(t)$ can be given by

$$\begin{aligned} \dot{e}_f(t) &= \dot{x}_f - \dot{\hat{x}}_f \\ &= \dot{x}_f - \dot{v}_c - L_c\dot{Q} \\ &= A_f x_f + B_f(x_r)\delta_e + F_f(x_r, \Phi) \\ &\quad -(A_f - L_c C_f)(v_c + L_c Q) - B_f(x_r)\delta_e \\ &\quad -F_f(x_r, \Phi) + L_c(f_4(x_r, \Phi) + g_4(x_r, \Phi)\delta_e) \\ &\quad -L_c(f_4(x_r, \Phi) + g_4(x_r, \Phi)\delta_e + C_f e_f(t)) \\ &= (A_f - L_c C_f)e_f(t). \end{aligned}$$

Thus, the differential equation for $e_f(t)$ is described as

$$\dot{e}_f(t) = \bar{A}_f e_f(t), \tag{13}$$

where $\bar{A}_f = A_f - L_c C_f$. The system (13) is asymptotically stable, if an observer gain L_c can be found such that $\bar{A}_f$ is a Hurwitz matrix.

When $A_f = 0$, $C_f = I$, $B_f(x_r) = 0$ and $F_f(x_r, \Phi) = 0$ (that is, $\dot{d}_c \equiv 0$), a simpler observer can be designed to estimate d_c as

$$\begin{cases} \hat{d}_c = z_d + L_d Q \\ \dot{z}_d = -L_d(z_d + L_d Q) - L_d(f_4(x_r, \Phi) \\ \qquad +g_4(x_r, \Phi)\delta_e), \end{cases} \tag{14}$$

where z_d and L_d are the internal state and the gain of observer (14), respectively. The observer (14) is similar to the disturbance observer presented in [22,27,35,36]. The estimation error using observer (14) can be reduced by increasing the observer gain L_d, if the disturbance is slowly time-varying. Another kind of disturbance observer presented in [12,37,38] were designed to estimate the disturbances that are generated by exogenous systems which are different from the disturbance d_c under consideration in this paper.

Remark 3 The moment of inertia $\bar{I}_{yy}$, interplay coupling parameter $\tilde{\psi}_i$, natural frequency ω_i, and damping ratio ζ_i can be worked out, if we know the mass, length, and rigidity of the vehicle. So the parameter matrices A_f and C_f can be obtained. In fact, the mass, length, and rigidity may have uncertainty in practice. Thus, a work is being done to design a robust coupling observer in order to estimate the disturbance d_c when the matrices A_f, $B_f(x_r)$, C_f and $F_f(x_r, \Phi)$ are uncertain.

Remark 4 In order to reject the disturbance d_c by using coupling-observer-based compensator later, the boundedness of d_c needs to be analyzed. Recall that $d_c = C_f x_f$, this problem turns to the boundedness analysis of x_f. First, Let us rewrite the model (11) as

$$\dot{x}_f = A_f x_f + w_f, \tag{15}$$

where $w_f = B_f(x_r)\delta_e + F_f(x_r, \Phi)$ is considered as an input of flexible system (15). Then the characteristic equation of A_f is

$$\det(\lambda I - A_f) = a_0\lambda^4 + a_1\lambda^3 + a_2\lambda^2 + a_3\lambda + a_4 = 0, \tag{16}$$

where $a_0 = 1$, $a_1 = 2(\bar{\zeta}_1\bar{\omega}_1 + \bar{\zeta}_2\bar{\omega}_2)$, $a_2 = \bar{\omega}_1^2 + \bar{\omega}_2^2 + 4\bar{p}\bar{\zeta}_1\bar{\omega}_1\bar{\zeta}_2\bar{\omega}_2$, $a_3 = 2\bar{p}\bar{\omega}_1\bar{\omega}_2(\bar{\zeta}_1\bar{\omega}_2 + \bar{\zeta}_2\bar{\omega}_1)$,

$a_4 = \bar{p}\bar{\omega}_1^2\bar{\omega}_2^2$, in which $\bar{\zeta}_1 = \sqrt{p_1}\zeta_1$, $\bar{\omega}_1 = \sqrt{p_1}\omega_1$, $\bar{\zeta}_2 = \sqrt{p_2}\zeta_2$, $\bar{\omega}_2 = \sqrt{p_2}\omega_2$, $\bar{p} = 1 - (p_3^2/(p_1 p_2))$. Obviously, $0 < \bar{p} < 1$. The Routh Table is described as

s^4	a_0	a_2	a_4
s^3	a_1	a_3	0
s^2	$(a_1a_2 - a_0a_3)/a_1$	a_4	0
s^1	$(a_1a_2a_3 - a_0a_3^2 - a_4a_1^2)/(a_1a_2 - a_0a_3)$	0	
s^0	a_4		

where

$$a_1a_2 - a_0a_3 = 2(1-\bar{p})(\bar{\zeta}_1\bar{\omega}_1\bar{\omega}_2^2 + \bar{\zeta}_2\bar{\omega}_2\bar{\omega}_1^2) + 2(\bar{\zeta}_1\bar{\omega}_1^3 \bar{\zeta}_2\bar{\omega}_2^3) + 8\bar{p}\bar{\zeta}_1\bar{\omega}_1\bar{\zeta}_2\bar{\omega}_2(\bar{\zeta}_1\bar{\omega}_1 + \bar{\zeta}_2\bar{\omega}_2),$$

$$a_1a_2a_3 - a_0a_3^2 - a_4a_1^2 = 4\bar{p}(1-\bar{p})(\bar{\zeta}_1\bar{\omega}_2 + \bar{\zeta}_2\bar{\omega}_1)^2 + 4\bar{p}\bar{\zeta}_1\bar{\omega}_1\bar{\zeta}_2\bar{\omega}_2(\bar{\omega}_1^2 - \bar{\omega}_2^2)^2 + 8\bar{\zeta}_1\bar{\omega}_1\bar{\zeta}_2\bar{\omega}_2(\bar{\zeta}_1\bar{\omega}_1 + \bar{\zeta}_2\bar{\omega}_2).$$

Observe that coefficients of the first column in Routh Table are all positive, when $\zeta_1 > 0$, $\zeta_2 > 0$, $\omega_1 > 0$ and $\omega_2 > 0$. Thus A_f is Hurwitz stable. The solution of state-space equation (15) is given by $x_f(t) = e^{A_f t}x_f(0) + \int_0^t e^{A_f(t-\tau)}w_f(\tau)\mathrm{d}\tau$, where w_f is bounded because the angle of attack α, the dynamic pressure q and the control inputs Φ and δ_e are all bounded for the flight control of cruising regimes. Therefore, the flexible state x_f and the disturbance d_c are bounded.

3.3 Nonlinear composite controller design

With the coupling observer (12), a nonlinear composite controller which combines a coupling-observer-based feedforward compensator and a dynamic-inversion-based feedback controller is constructed in this subsection. Let us consider the following second-order actuator model, which is appended to the input Φ.

$$\ddot{\Phi} = -2\zeta\omega\dot{\Phi} - \omega^2\Phi + \omega^2\Phi_c. \tag{17}$$

By combing with (7)–(10) and selecting $\bar{u} = [\delta_e \ \ \Phi_c]^T$ as the new control input, a six dimension model with full vector relative degree can be obtained to design a dynamic-inversion-based feedback controller. From (7)-(10) and (17), the third differential of V and γ can be obtained as follows:

$$\dddot{V} = (\partial f_1(x_r, \Phi)/\partial x)\ddot{x} + \dot{x}^T(\partial^2 f_1(x_r, \Phi)/\partial x^2)\dot{x} \tag{18}$$

$$\dddot{\gamma} = (\partial f_3(x_r, \Phi)/\partial x)\ddot{x} + \dot{x}^T(\partial^2 f_3(x_r, \Phi)/\partial x^2)\dot{x}, \tag{19}$$

where $x = [V \ \ \alpha \ \ \gamma \ \ \Phi]^T$, $\dot{x} = [\dot{V} \ \ \dot{\alpha} \ \ \dot{\gamma} \ \ \dot{\Phi}]^T$, and $\ddot{x} = [\ddot{V} \ \ \ddot{\alpha} \ \ \ddot{\gamma} \ \ \ddot{\Phi}]^T$. Because $\dot{x}$ and $\ddot{x}$ contain the functions about control input $\bar{u}$ and disturbance d_c, the expressions of $\dddot{V}$ and $\dddot{\gamma}$ can be rewritten as

$$\begin{bmatrix} \dddot{V} \\ \dddot{\gamma} \end{bmatrix} = \begin{bmatrix} f_V(x_r, \Phi) \\ f_\gamma(x_r, \Phi) \end{bmatrix} + \begin{bmatrix} g_{V1}(x_r, \Phi) & g_{V2}(x_r, \Phi) \\ g_{\gamma 1}(x_r, \Phi) & g_{\gamma 2}(x_r, \Phi) \end{bmatrix}\bar{u} + \begin{bmatrix} g_{V3}(x_r, \Phi) \\ g_{\gamma 3}(x_r, \Phi) \end{bmatrix} d_c, \tag{20}$$

where

$$f_V(x_r, \Phi) = \pi^V\ddot{x}_0 + \dot{x}_0^T\Pi^V\dot{x}_0,$$

$$g_{V1}(x_r, \Phi) = \frac{g_4(x_r, \Phi)}{m}\left(\frac{\partial T}{\partial \alpha}\cos\alpha - T\sin\alpha - \frac{\partial \bar{D}}{\partial \alpha}\right),$$

$$g_{V2}(x_r, \Phi) = \frac{\omega^2}{m}\left(\frac{\partial T}{\partial \Phi}\cos\alpha\right),$$

$$g_{V3}(x_r, \Phi) = \frac{1}{m}\left(\frac{\partial T}{\partial \alpha}\cos\alpha - T\sin\alpha - \frac{\partial \bar{D}}{\partial \alpha}\right),$$

$$f_\gamma(x_r, \Phi) = \pi^\gamma\ddot{x}_0 + \dot{x}_0^T\Pi^\gamma\dot{x}_0,$$

$$g_{\gamma 1}(x_r, \Phi) = \frac{g_4(x_r, \Phi)}{mV}\left(\frac{\partial T}{\partial \alpha}\sin\alpha + T\cos\alpha + \frac{\partial \bar{L}}{\partial \alpha}\right),$$

$$g_{\gamma 2}(x_r, \Phi) = \frac{\omega^2}{mV}\left(\frac{\partial T}{\partial \Phi}\sin\alpha\right),$$

$$g_{\gamma 3}(x_r, \Phi) = \frac{1}{mV}\left(\frac{\partial T}{\partial \alpha}\sin\alpha + T\cos\alpha + \frac{\partial \bar{L}}{\partial \alpha}\right),$$

in which

$$\dot{x}_0 = \begin{bmatrix} f_1(x_r, \Phi) \\ f_2(x_r, \Phi) \\ f_3(x_r, \Phi) \\ \dot{\Phi} \end{bmatrix}, \ \ddot{x}_0 = \begin{bmatrix} \pi^V\dot{x}_0 \\ -\pi^\gamma\dot{x}_0 + f_4(x_r, \Phi) \\ \pi^\gamma\dot{x}_0 \\ -2\zeta\omega\dot{\Phi} - \omega^2\Phi \end{bmatrix},$$

$$\pi^V = \partial f_1(x_r, \Phi)/\partial x, \ \pi^\gamma = \partial f_3(x_r, \Phi)/\partial x,$$

$$\Pi^V = \partial^2 f_1(x_r, \Phi)/\partial x^2, \ \Pi^\gamma = \partial^2 f_3(x_r, \Phi)/\partial x^2.$$

The detailed expressions of π^V, π^γ, Π^V, and Π^γ are given in the Appendix. It is observed that the nonlinear functions $f_V(x_r, \Phi)$, $f_\gamma(x_r, \Phi)$, $g_{Vj}(x_r, \Phi)$, and $g_{\gamma j}(x_r, \Phi)$, $j = 1, 2, 3$ are sufficiently smooth with respect to x_r and Φ.

Next, we begin to design the nonlinear composite controller based on the coupling observer. Using the estimate $\hat{d}_c$ produced by observer (12), the composite controller can be designed as

$$\bar{u} = u_1 + u_2 + u_3, \tag{21}$$

where

$$u_1 = -G(x_r,\Phi)^{-1}\begin{bmatrix} f_V(x_r,\Phi) \\ f_\gamma(x_r,\Phi)\end{bmatrix},$$
$$u_2 = -G(x_r,\Phi)^{-1}\begin{bmatrix} -\ddot{V}_d+\upsilon_1 \\ -\ddot{\gamma}_d+\upsilon_2\end{bmatrix},$$
$$u_3 = -G(x_r,\Phi)^{-1}\begin{bmatrix} g_{V3}(x_r,\Phi) \\ g_{\gamma 3}(x_r,\Phi)\end{bmatrix}\hat{d}_c,$$
$$G(x_r,\Phi) = \begin{bmatrix} g_{V1}(x_r,\Phi) & g_{V2}(x_r,\Phi) \\ g_{\gamma 1}(x_r,\Phi) & g_{\gamma 2}(x_r,\Phi)\end{bmatrix},$$
$$\upsilon_1 = k_{V4}\ddot{e}_V(t)+k_{V3}\dot{e}_V(t)+k_{V2}e_V(t) + k_{V1}\int_0^t e_V(\tau)\mathrm{d}\tau,$$
$$\upsilon_2 = k_{\gamma 4}\ddot{e}_\gamma(t)+k_{\gamma 3}\dot{e}_\gamma(t)+k_{\gamma 2}e_\gamma(t) + k_{\gamma 1}\int_0^t e_\gamma(\tau)\mathrm{d}\tau,$$

in which $e_V(t) = V - V_d$ and $e_\gamma(t) = \gamma - \gamma_d$ are tracking errors of velocity and flight-path angle, respectively. The control gains $K_V = -[k_{V1}\ \ k_{V2}\ \ k_{V3}\ \ k_{V4}]$ and $K_\gamma = -[k_{\gamma 1}\ \ k_{\gamma 2}\ \ k_{\gamma 3}\ \ k_{\gamma 4}]$ are to be obtained by solving Riccati equations in the following.

Remark 5 The control law (21) includes three parts: the first term is designed to compensate the nonlinear functions $f_V(x_r,\Phi)$ and $f_\gamma(x_r,\Phi)$, the second term is designed to track the desired signals V_d and γ_d, and the third term is designed to reject the disturbance d_c. The dynamic-inversion-based feedback controller is composed of the first and the second parts, while the coupling-observer-based feedforward compensator is the third part.

Remark 6 When $\hat{d}_c \equiv 0$, that is, there is no coupling compensation, the nonlinear composite controller (21) obviously becomes the dynamic-inversion-based nonlinear controller presented in [29], which is written as

$$\bar{u} = \bar{u}_1 + \bar{u}_2, \tag{22}$$

where

$$\bar{u}_1 = -\bar{G}(x_r,\Phi)^{-1}\begin{bmatrix} \bar{f}_V(x_r,\Phi) \\ \bar{f}_\gamma(x_r,\Phi)\end{bmatrix},$$
$$\bar{u}_2 = -\bar{G}(x_r,\Phi)^{-1}\begin{bmatrix} -\ddot{V}_d+\upsilon_1 \\ -\ddot{\gamma}_d+\upsilon_2\end{bmatrix},$$

in which

$$\bar{G}(x_r,\Phi) = \begin{bmatrix} \bar{g}_{V1}(x_r,\Phi) & g_{V2}(x_r,\Phi) \\ \bar{g}_{\gamma 1}(x_r,\Phi) & g_{\gamma 2}(x_r,\Phi)\end{bmatrix},$$
$$\ddot{\bar{x}}_0 = \begin{bmatrix} \pi^V\dot{x}_0 \\ -\pi^\gamma\dot{x}_0+\bar{f}_4(x_r,\Phi) \\ \pi^\gamma\dot{x}_0 \\ -2\zeta\omega\dot{\Phi}-\omega^2\Phi\end{bmatrix},$$
$$\bar{f}_V(x_r,\Phi) = \pi^V\ddot{\bar{x}}_0+\dot{x}_0^T\Pi^V\dot{x}_0,$$
$$\bar{g}_{V1}(x_r,\Phi) = \frac{\bar{g}_4(x_r,\Phi)}{m}\left(\frac{\partial T}{\partial\alpha}\cos\alpha - T\sin\alpha - \frac{\partial\bar{D}}{\partial\alpha}\right),$$
$$\bar{f}_\gamma(x_r,\Phi) = \pi^\gamma\ddot{\bar{x}}_0+\dot{x}_0^T\Pi^\gamma\dot{x}_0,$$
$$\bar{g}_{\gamma 1}(x_r,\Phi) = \frac{\bar{g}_4(x_r,\Phi)}{mV}\left(\frac{\partial T}{\partial\alpha}\sin\alpha + T\cos\alpha + \frac{\partial\bar{L}}{\partial\alpha}\right),$$
$$\bar{f}_4(x_r,\Phi) = \bar{I}_{yy}^{-1}[z_T T + qS\bar{c}(C_M^{\alpha^2}\alpha^2 + C_M^\alpha\alpha + C_M^0)],$$
$$\bar{g}_4(x_r,\Phi) = \bar{I}_{yy}^{-1}qS\bar{c}C_M^{\delta_e}.$$

Remark 7 Note that the non-singular conditions for $G(x_r,\Phi)$ and $\bar{G}(x_r,\Phi)$ can be represented as

$$\det[G(x_r,\Phi)] \neq 0 \Longleftrightarrow$$
$$\tfrac{\omega^2}{m^2V}\tfrac{\partial T}{\partial\Phi}g_4(x_r,\Phi)(T+\tfrac{\partial\bar{D}}{\partial\alpha}\sin\alpha+\tfrac{\partial\bar{L}}{\partial\alpha}\cos\alpha)\neq 0,$$
$$\det[\bar{G}(x_r,\Phi)] \neq 0 \Longleftrightarrow$$
$$\tfrac{\omega^2}{m^2V}\tfrac{\partial T}{\partial\Phi}\bar{g}_4(x_r,\Phi)(T+\tfrac{\partial\bar{D}}{\partial\alpha}\sin\alpha+\tfrac{\partial\bar{L}}{\partial\alpha}\cos\alpha)\neq 0.$$

In [29], the matrix $\bar{G}(x_r,\Phi)$ has been verified to be nonsingular over the operating range of interest, which is the range of parameter values used in the curve fits. Thus $(T+\frac{\partial\bar{D}}{\partial\alpha}\sin\alpha+\frac{\partial\bar{L}}{\partial\alpha}\cos\alpha)\neq 0$ holds due to $\frac{\omega^2}{m^2V}\frac{\partial T}{\partial\Phi}\bar{g}_4(x_r,\Phi)\neq 0$. Moreover, $\frac{\omega^2}{m^2V}\frac{\partial T}{\partial\Phi}g_4(x_r,\Phi)\neq 0$ also holds for the dynamic pressure q considered in this paper. Finally, the $\frac{\omega^2}{m^2V}\frac{\partial T}{\partial\Phi}g_4(x_r,\Phi)(T+\frac{\partial\bar{D}}{\partial\alpha}\sin\alpha+\frac{\partial\bar{L}}{\partial\alpha}\cos\alpha)\neq 0$ holds, that is, the matrix $G(x_r,\Phi)$ is also nonsingular.

Remark 8 The gains (K_V and K_γ) of controller (22) are designed using LQR in [29], which obtained by solving two Riccati equations. In order to compare controller (21) with controller (22) clearly, the gains (L_c, K_V and K_γ) of controller (21) are also related with the solutions of Riccati equations detailed in the following.

Considering (13) and substituting (21) into (20), a composite closed-loop system can be obtained as follows:

$$\begin{cases}\dot{e}_f(t) = \bar{A}_f e_f(t) \\ \dot{\bar{e}}_V(t) = \bar{A}_V\bar{e}_V(t)+\bar{B}_V C_f e_f(t) \\ \dot{\bar{e}}_\gamma(t) = \bar{A}_\gamma\bar{e}_\gamma(t)+\bar{B}_\gamma C_f e_f(t),\end{cases} \tag{23}$$

where $\bar{A}_V = A_0 + B_0 K_V$, $\bar{A}_\gamma = A_0 + B_0 K_\gamma$, $\bar{B}_V = g_{V3}(x_r, \Phi) B_0$, $\bar{B}_\gamma = g_{\gamma 3}(x_r, \Phi) B_0$,

$$\bar{e}_V(t) = \begin{bmatrix} \int_0^t e_V(\tau)\mathrm{d}\tau \\ e_V(t) \\ \dot{e}_V(t) \\ \ddot{e}_V(t) \end{bmatrix}, \quad \bar{e}_\gamma(t) = \begin{bmatrix} \int_0^t e_\gamma(\tau)\mathrm{d}\tau \\ e_\gamma(t) \\ \dot{e}_\gamma(t) \\ \ddot{e}_\gamma(t) \end{bmatrix},$$

$$A_0 = \begin{bmatrix} 0 & 1 & 0 & 0 \\ 0 & 0 & 1 & 0 \\ 0 & 0 & 0 & 1 \\ 0 & 0 & 0 & 0 \end{bmatrix}, \quad B_0 = \begin{bmatrix} 0 \\ 0 \\ 0 \\ 1 \end{bmatrix}.$$

The composite closed-loop system (23) can be described compactly as

$$\dot{e}(t) = Ae(t), \tag{24}$$

where

$$e(t) = \begin{bmatrix} e_f(t) \\ \bar{e}_V(t) \\ \bar{e}_\gamma(t) \end{bmatrix}, \quad A = \begin{bmatrix} \bar{A}_f & 0 & 0 \\ \bar{B}_V C_f & \bar{A}_V & 0 \\ \bar{B}_\gamma C_f & 0 & \bar{A}_\gamma \end{bmatrix}.$$

To design the gains of controller (21) and analyze the stability of composite system (24), the following assumption is needed in this paper. The assumption can be satisfied for the hypersonic cruising regimes.

Assumption 1 Nonlinear functions $g_{V3}(x_r, \Phi)$ and $g_{\gamma 3}(x_r, \Phi)$ are bounded, that is, $||g_{V3}(x_r, \Phi)|| \le \sigma_{V3}$, $||g_{\gamma 3}(x_r, \Phi)|| \le \sigma_{\gamma 3}$, where σ_{V3} and $\sigma_{\gamma 3}$ are all known positive constants.

Theorem 1 *Considering the closed-loop system (24), for $\beta_V > 0$ and $\beta_\gamma > 0$, if there exist three positive definite matrices, $P_1 \in \mathcal{R}^{4\times4}$, $P_2 \in \mathcal{R}^{4\times4}$ and $P_3 \in \mathcal{R}^{4\times4}$, satisfying the following Riccati equations:*

$$P_1 A_f^T + A_f P_1 - P_1 C_f^T R_f^{-1} C_f P_1 + Q_f = 0, \tag{25}$$

$$P_2 A_0 + A_0^T P_2 - P_2 B_0 R_V^{-1} B_0^T P_2 + Q_V = 0, \tag{26}$$

$$P_3 A_0 + A_0^T P_3 - P_3 B_0 R_\gamma^{-1} B_0^T P_3 + Q_\gamma = 0, \tag{27}$$

and the weights $Q_f \in \mathcal{R}^{4\times4}$, $Q_V \in \mathcal{R}^{4\times4}$, $Q_\gamma \in \mathcal{R}^{4\times4}$, $R_f \in \mathcal{R}$, $R_V \in \mathcal{R}$ and $R_\gamma \in \mathcal{R}$, satisfying

$$Q_f \ge (\beta_V^{-2}\sigma_{V3}^2 + \beta_\gamma^{-2}\sigma_{\gamma 3}^2) C_f^T C_f, \quad Q_V \ge 0,$$

$$Q_\gamma \ge 00 < R_f, \quad 0 < R_V \le \beta_V^{-2}, \quad 0 < R_\gamma \le \beta_\gamma^{-2}$$

then by selecting $L_c^T = R_f^{-1} C_f P_1$, $K_V = -R_V^{-1} B_0^T P_2$ and $K_\gamma = -R_\gamma^{-1} B_0^T P_3$, the composite closed-loop system (24) is asymptotically stable.

Proof A Lyapunov function candidate for the system (24) is chosen as

$$W(t) = e^T(t) P e(t),$$

where $P = \mathrm{diag}\{\bar{P}_1, P_2, P_3\}$ and $\bar{P}_1 = P_1^{-1}$. The derivative of $W(t)$ along trajectories of system (24) can be written as

$$\begin{aligned} \dot{W}(t) &= e^T(t)(PA + A^T P)e(t) \\ &= e^T(t)\bar{\Gamma}e(t) - e^T(t)\chi_1^T\chi_1 e(t) - e^T(t)\chi_2^T\chi_2 e(t) \\ &\le e^T(t)\bar{\Gamma}e(t), \end{aligned}$$

where $\bar{\Gamma} = \mathrm{diag}\{\bar{\Gamma}_1, \bar{\Gamma}_2, \bar{\Gamma}_3\}$, $\chi_1 = [\beta_V^{-1} g_{V3}(x_r, \Phi) C_f \ -\beta_V B_0^T P_2 \ 0]$, $\chi_2 = [\beta_\gamma^{-1} g_{\gamma 3}(x_r, \Phi) C_f \ 0 \ -\beta_\gamma B_0^T P_3]$, in which

$$\begin{aligned} \bar{\Gamma}_1 &= \bar{A}_f^T \bar{P}_1 + \bar{P}_1 \bar{A}_f + [\beta_V^{-2} g_{V3}^2(x_r, \Phi) \\ &\quad + \beta_\gamma^{-2} g_{\gamma 3}^2(x_r, \Phi)] C_f^T C_f, \\ \bar{\Gamma}_2 &= \bar{A}_V^T P_2 + P_2 \bar{A}_V + P_2 B_0 \beta_V^2 B_0^T P_2, \\ \bar{\Gamma}_3 &= \bar{A}_\gamma^T P_3 + P_3 \bar{A}_\gamma + P_3 B_0 \beta_\gamma^2 B_0^T P_3. \end{aligned}$$

According to Assumption 1, we know that

$$\beta_V^{-2} g_{V3}^2(x_r, \Phi) + \beta_\gamma^{-2} g_{\gamma 3}^2(x_r, \Phi) \le \beta_V^{-2}\sigma_{V3}^2 + \beta_\gamma^{-2}\sigma_{\gamma 3}^2.$$

Therefore

$$\dot{W}(t) \le e^T(t)\Gamma e(t), \tag{28}$$

where the matrix $\Gamma = \mathrm{diag}\{\bar{A}_f^T \bar{P}_1 + \bar{P}_1 \bar{A}_f + (\beta_V^{-2}\sigma_{V3}^2 + \beta_\gamma^{-2}\sigma_{\gamma 3}^2) C_f^T C_f, \ \bar{A}_V^T P_2 + P_2 \bar{A}_V + P_2 B_0 \beta_V^2 B_0^T P_2, \ \bar{A}_\gamma^T P_3 + P_3 \bar{A}_\gamma + P_3 B_0 \beta_\gamma^2 B_0^T P_3\}$. Pre- and post-multiply the inequality (28) by $\mathrm{diag}\{P_1, I, I\}$ and substituting matrices Γ, $\bar{A}_f$, $\bar{A}_V$ and $\bar{A}_\gamma$ into the inequality, we obtain

$$\begin{aligned} \dot{W}(t) \le\ & e_f^T(t)(P_1 A_f^T + A_f P_1 - P_1 C_f^T L_c^T - L_c C_f P_1 \\ & + (\beta_V^{-2}\sigma_{V3}^2 + \beta_\gamma^{-2}\sigma_{\gamma 3}^2) C_f^T C_f) e_f(t) + \bar{e}_V^T(t) \\ & (A_V^T P_2 + P_2 A_V + K_V^T B_0^T P_2 + P_2 B_0 K_V \\ & + P_2 B_0 \beta_V^2 B_0^T P_2)\bar{e}_V(t) + \bar{e}_\gamma^T(t)(A_\gamma^T P_3 + P_3 A_\gamma \\ & + K_\gamma^T B_0^T P_3 + P_3 B_0 K_\gamma + P_3 B_0 \beta_\gamma^2 B_0^T P_3)\bar{e}_\gamma(t). \end{aligned}$$

If the matrices P_1, P_2 and P_3 are the solutions of the Riccati equations (25)–(27) and the gains of controller (21) are chosen as $L_c^T = R_f^{-1} C_f P_1$, $K_V = -R_V^{-1} B_0^T P_2$ and $K_\gamma = -R_\gamma^{-1} B_0^T P_3$, we obtain

$$\begin{aligned} \dot{W}(t) \le\ & e_f^T(t)(-P_1 C_f^T R_f^{-1} C_f P_1 - Q_f + (\beta_V^{-2}\sigma_{V3}^2 \\ & + \beta_\gamma^{-2}\sigma_{\gamma 3}^2) C_f^T C_f) e_f(t) + \bar{e}_V^T(t)(-P_2 B_0 R_V^{-1} \\ & B_0^T P_2 - Q_V + P_2 B_0 \beta_V^2 B_0^T P_2)\bar{e}_V(t) + \bar{e}_\gamma^T(t) \\ & (-P_3 B_0 R_\gamma^{-1} B_0^T P_3 - Q_\gamma + P_3 B_0 \beta_\gamma^2 B_0^T P_3)\bar{e}_\gamma(t). \end{aligned}$$

When the weights Q_f, Q_V, Q_γ R_f, R_V and R_γ satisfy the following conditions:

$$Q_f \geq (\beta_V^{-2}\sigma_{V3}^2 + \beta_\gamma^{-2}\sigma_{\gamma 3}^2)C_f^T C_f, \quad Q_V \geq 0,$$
$$Q_\gamma \geq 0, 0 < R_f, \quad 0 < R_V \leq \beta_V^{-2}, \quad 0 < R_\gamma \leq \beta_\gamma^{-2},$$

the $\dot{W}(t) < 0$, that is, the composite closed-loop system (24) is asymptotically stable. □

Remark 9 The gains (L_c, K_V and K_γ) of controller (21) can be adjusted to improve the estimation performance and control performance by choosing appropriate values of weights (Q_f, Q_V, Q_γ, R_f, R_V and R_γ) and positive parameters (β_V and β_γ).

4 Simulations

In this section, the effectiveness of the proposed method is demonstrated by numerical simulations. To compare with the controller (21), the controller (22) will be also applied for the flight control of FAHVs. For simplification, the controllers (21) and (22) are called as controller 1 and controller 2, respectively. The simulation results are obtained for the full nonlinear model of FAHVs with the elevator-to-lift coupling and rigid-flexible coupling. The values of rigid-body state and flexible state at trimmed cruise condition, the vehicle parameters (that is, I_{yy}, m, ρ, S, $\bar{c}$) and the coefficients that appear in the forces and moment (that is, $C_M^{(\cdot)}$, $C_T^{(\cdot)}$, $C_{N_i}^{(\cdot)}$, $C_L^{(\cdot)}$, $C_D^{(\cdot)}$) are given in [29].

In the simulation, the FAHV needs to complete the same maneuver tasks as [29]. The selected reference trajectory begin at $q = 2,000\,\mathrm{lb\,ft^{-2}}$ and $h = 85,000$ ft. The aircraft climbs at a steady $50\,\mathrm{ft\,s^{-1}}$, while maintaining a constant dynamic pressure. Once the FAHV reaches Mach 10 at time 220 s, the Mach number is held constant at climb rate increase to $139\,\mathrm{ft\,s^{-1}}$ until leveling off at 115,000 ft. With above maneuver tasks, the desired signals $V_d(t)$ and $\gamma_d(t)$ can be obtained shown in Fig. 1a, b by using the relationships $q_d(t) = 0.5\rho_0 V_d^2(t)\exp(-(h_d(t) - h_0)/h_s)$, $M_a = V_d(t)/(20\sqrt{T_e})$ and $\dot{h}_d(t) = V_d(t)\sin(\gamma_d(t))$, where $q_d(t)$ and $h_d(t)$ are the desired signals of dynamic pressure and altitude, M_a and T_e denote Mach number and air temperature, respectively.

In order to fully analyze the performances of controller 1 and controller 2, two case studies will be considered. In the first case, controller 1 and controller 2 choose the same gains K_V and K_γ to analyze the effects caused by the disturbance d_c. In the second case, the different gain K_γ is chosen to compare the performance of the two controllers.

The first case sets weights $Q_f = 4.225 \times 10^5 C_f^T C_f$, $Q_V = \mathrm{diag}\{1,\ 10,\ 1,\ 1\}$, $Q_\gamma = I_{4\times 4}$, $R_f = 200$, $R_V = 1$, $R_\gamma = 0.1$, and parameters $\beta_V = 1$, $\beta_\gamma = 1$. Then we have $K_V = -[3.4849\ \ 5.5722\ \ 4.5983\ \ 1]$, $K_\gamma = -[5.4399\ \ 9.7962\ \ 8.4827\ \ 3.1623]$ and $L_c = [11.6038\ \ -7.2228\ \ -1.4551\ \ -1.6087]^T$ according to Theorem 1.

The simulation results of rigid-body state, control input, flexible state and disturbance d_c under controller 1 and controller 2 with the same gains K_V and K_γ are shown in Figs. 1, 2, 3, and 4. It can be seen from Fig. 1 that the tracking performances of controller 1 are similar to the ones of controller 2 due to choosing the same gains K_V and K_γ. However, there are oscillations in the simulation results of tracking errors, angle of attack, pitch rate, control input and flexible state using controller 2 shown in Figs. 1, 2, and 3. It can be observed from Fig. 4a that the simulation results of disturbance d_c under controller 2 also has high-frequency oscillation. Thus, the oscillations that appear in rigid-body variables, control input and flexible state are all caused by the disturbance d_c. Furthermore, the oscillations will be intensified, if the smaller tracking error of flight-path angle is needed for controller 2. Meanwhile, it also can be seen from Figs. 1, 2, 3, and 4 that the controller 1 with the same tracking performance as controller 2 can avoid these oscillations by using the coupling-observer-based compensator which is able to reject the disturbance d_c.

The vehicle may be out of control due to the high-frequency oscillation of elevator deflection δ_e. The durable oscillations appeared in flexible state may cause vehicle damage. Therefore, the oscillations produced by using controller 2 in the first case are undesired in practice. Thus the bigger weight R_γ of controller 2 (that is, $R_\gamma = 1$) is chosen in the second case study to reduce the oscillations, while the smaller weight R_γ (that is, $R_\gamma = 0.08$) is chosen to further improve the tracking performance of controller 1. So the new gain K_γ can be worked out as $K_\gamma = -[5.8258\ \ 10.7200\ \ 9.3979\ \ 3.5355]$ for controller 1 and $K_\gamma = -[3.0777\ \ 4.2361\ \ 3.0777\ \ 1]$ for controller 2. Other gains of controller 1 and controller 2 are same as the first case.

The simulation results of rigid-body state, control input, flexible state and disturbance d_c under controller

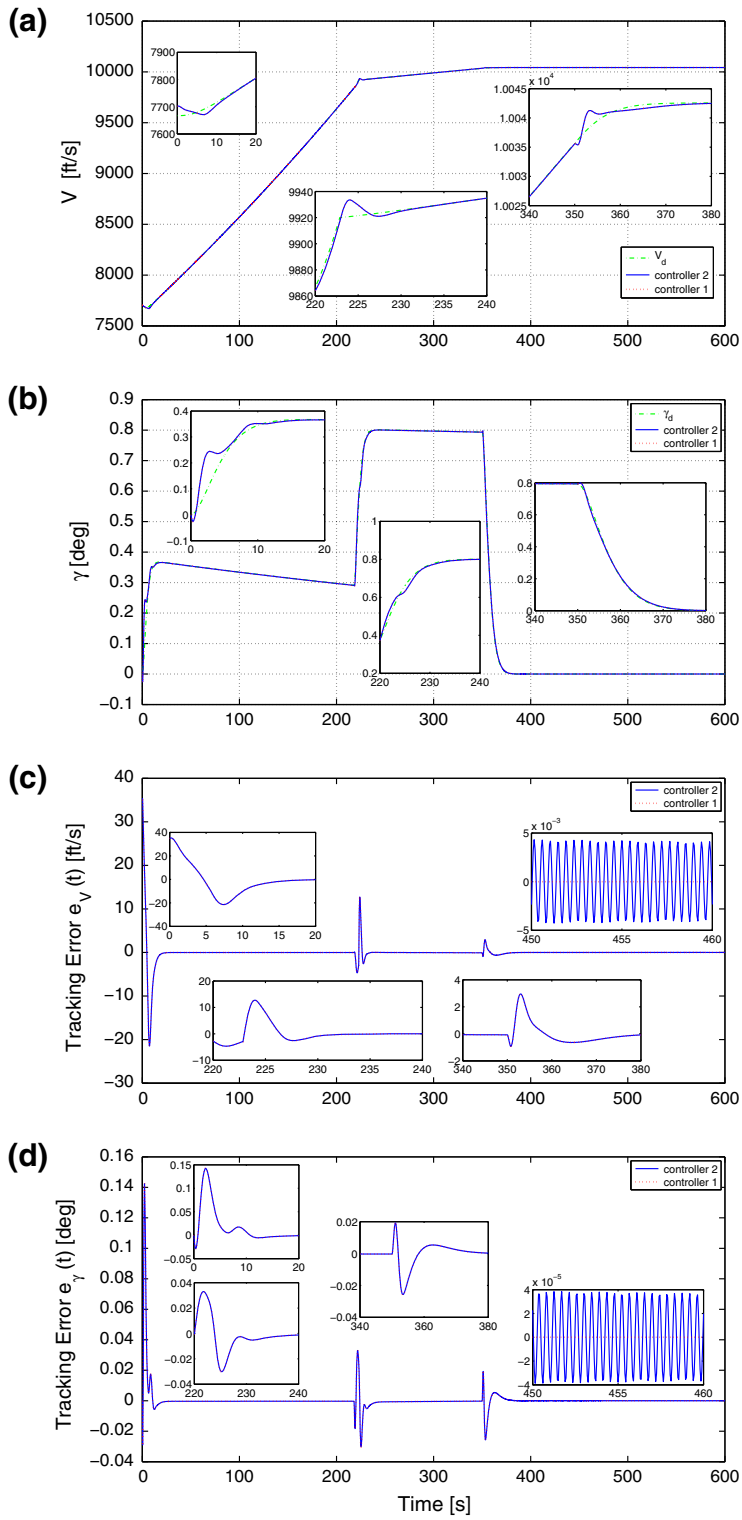

Fig. 1 Case study 1: **a** velocity $V(t)$ and desired trajectory $V_d(t)$, **b** flight path angle $\gamma(t)$ and desired trajectory $\gamma_d(t)$, **c** velocity tracking error $e_V(t)$, **d** flight-path angle tracking error $e_\gamma(t)$

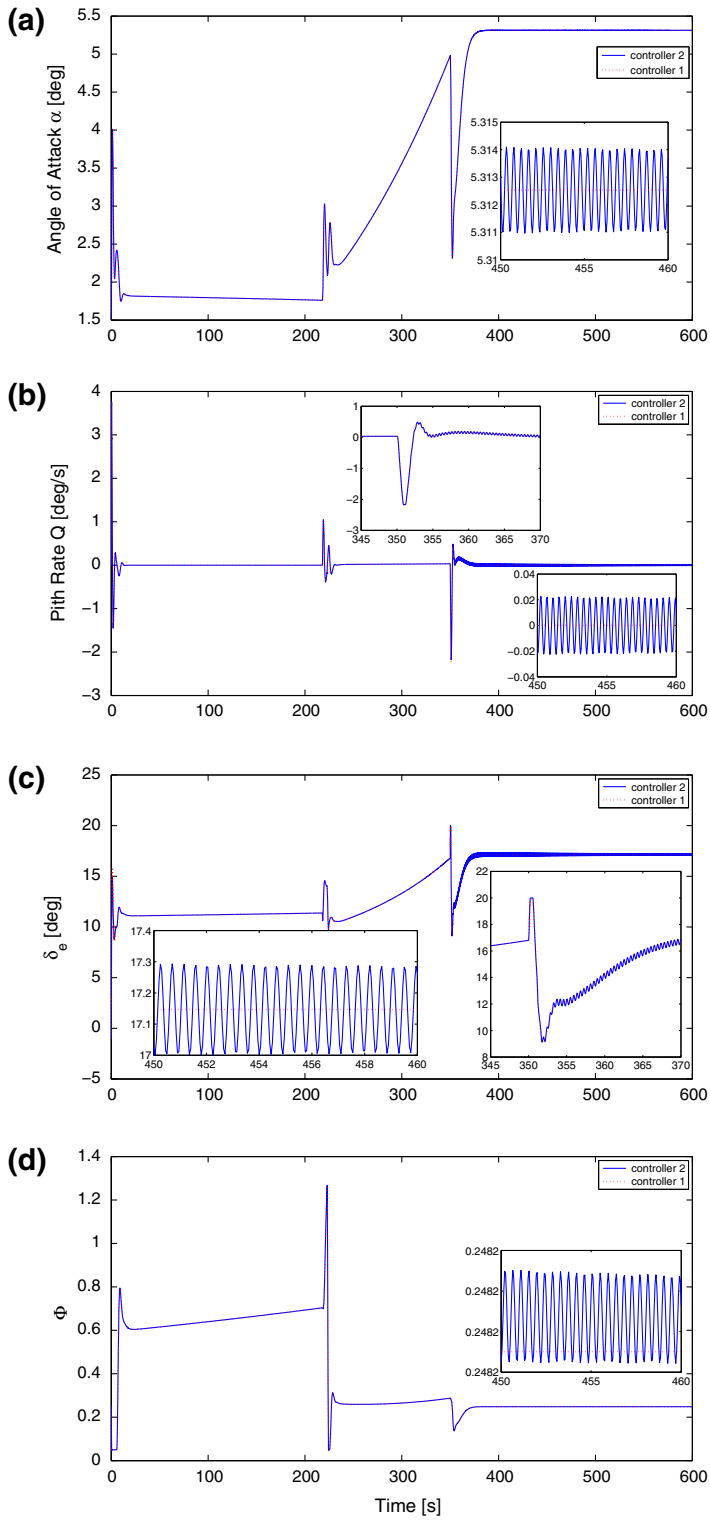

Fig. 2 Case study 1: **a** angle of attack $\alpha(t)$, **b** pitch rate $Q(t)$, **c** elevator deflection $\delta_e(t)$, **d** fuel equivalence ratio $\Phi(t)$

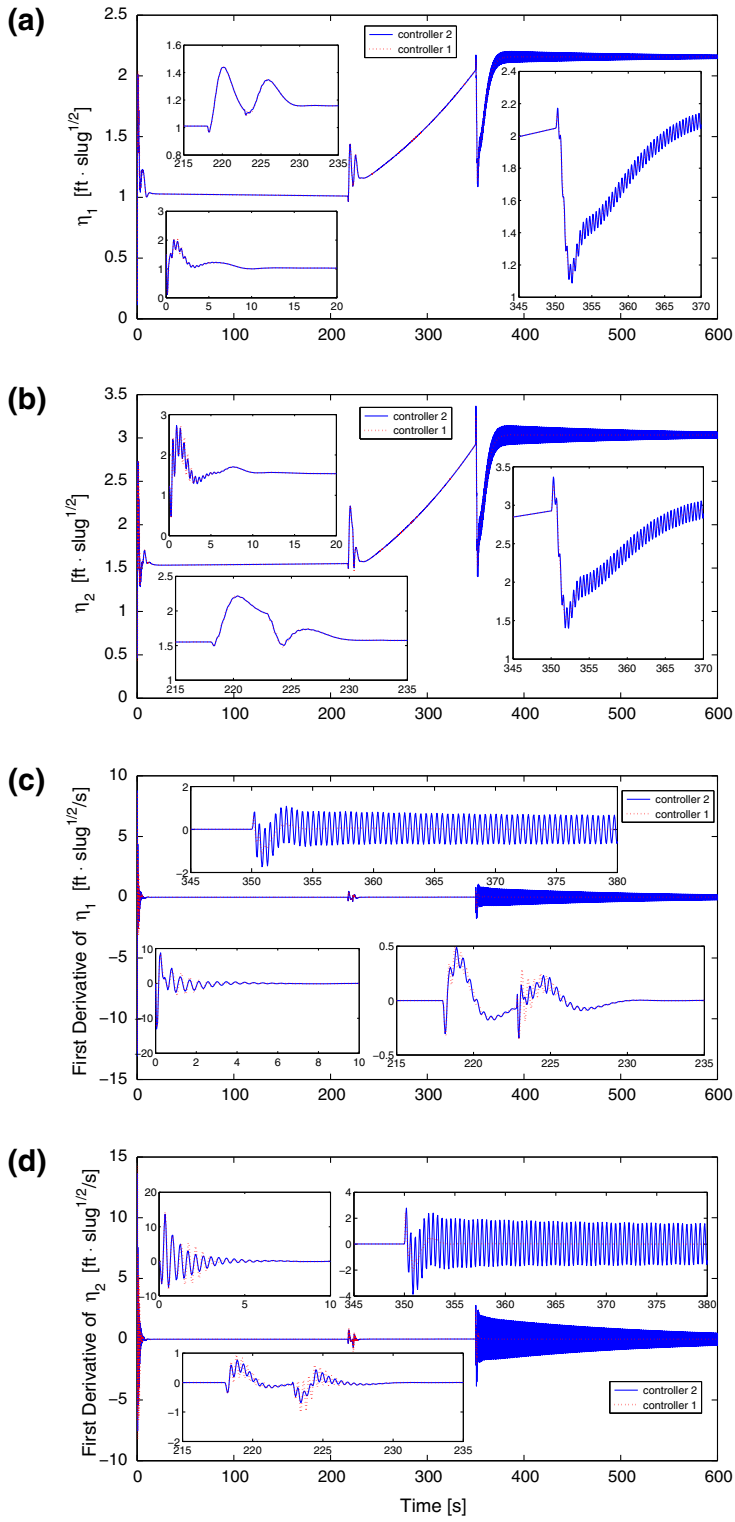

Fig. 3 Case study 1: **a** flexible mode $\eta_1(t)$, **b** flexible mode $\eta_2(t)$, **c** $\dot{\eta}_1(t)$, **d** $\dot{\eta}_2(t)$

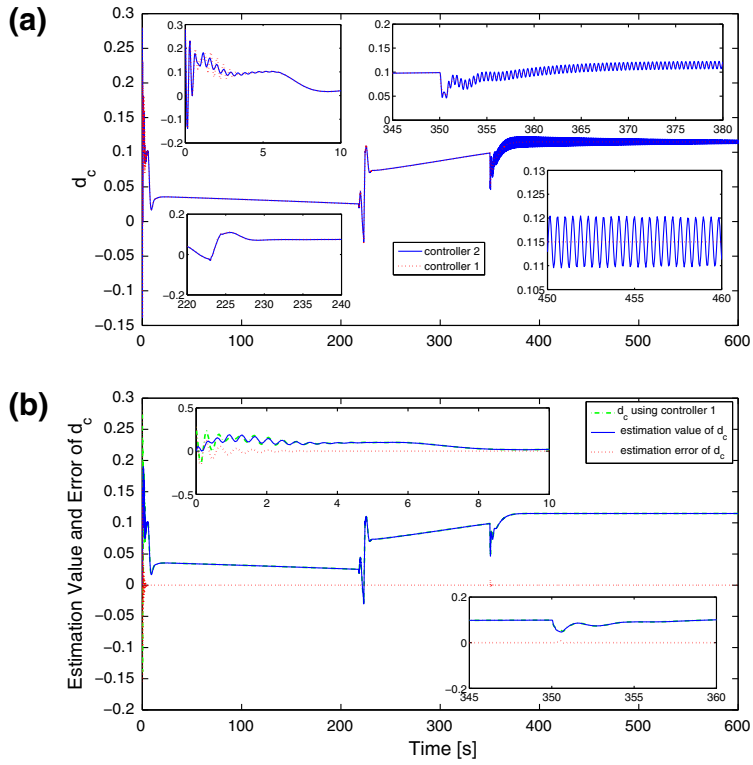

Fig. 4 Case study 1: **a** disturbance d_c, **b** estimation value and error of d_c

1 and controller 2 with different gain K_γ are shown in Figs. 5, 6, 7, and 8. It can be seen from Figs. 5, 6, 7, and 8 that the oscillations of tracking errors, angle of attack, pitch rate, control input, flexible state and disturbance are reduced in the simulation results using controller 2, but the tracking performance of controller 2 is degraded (that is, the tracking error of fight-path angle using controller 2 is bigger than the one using controller 1). Moreover, even if the smaller weight R_γ is chosen, there are no durable or high-frequency oscillations in the simulation results under controller 1. In addition, it can be seen from Figs. 4b and 8b that the disturbance d_c using controller 1 can be estimated very well by the coupling observer in the two case studies.

In a word, it may cause degradation of control performance or oscillations of control input and flexible state using controller 2 without considering the rigid-flexible couplings, while the controller 1 proposed in this paper can avoid these problems. That is, the tracking performances can be improved by using controller 1 compared with controller 2.

5 Conclusion

In this paper, the flexible effects produced by rigid-flexible coupling dynamics between flexible and rigid-body variables of FAHVs are formulated as a kind of disturbance. First, a control-design model with rigid-flexible coupling dynamics is given. And then, the nonlinear composite controller which combines a coupling-observer-based feedforward compensator and a dynamic-inversion-based feedback controller is presented, where the feedforward compensator is constructed to reject the flexible effects on pitch rate and the feedback controller is designed to guarantee velocity and flight-path angle track the desired signals. Simulation results show that it may cause degradation of control performance or high-frequency oscillations of control input and flexible state using the traditional nonlinear controller without considering the rigid-flexible couplings, while the coupling-observer-based controller can avoid these problems. In other words, the tracking performances can be improved by using the proposed composite controller compared with

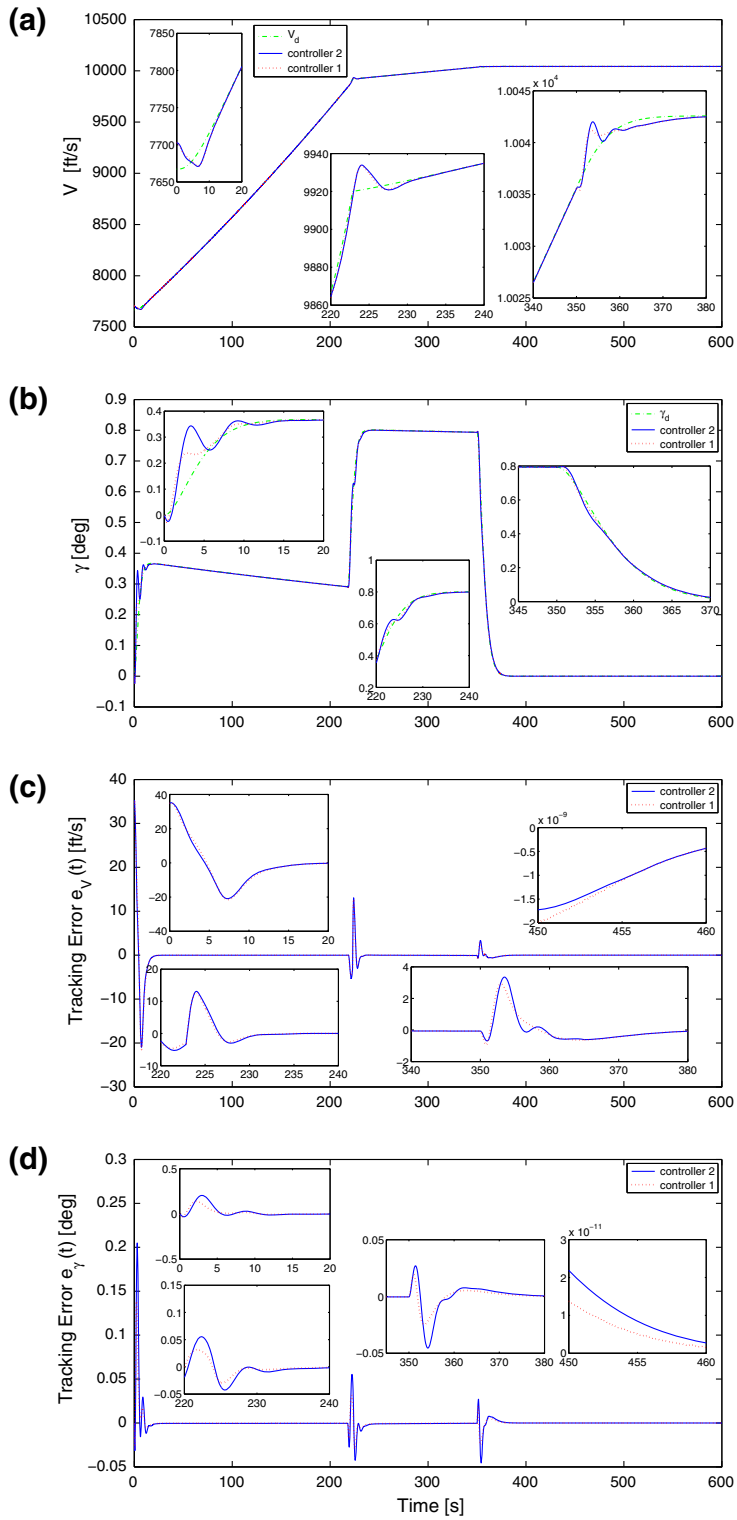

Fig. 5 Case study 2: **a** velocity $V(t)$ and desired trajectory $V_d(t)$, **b** flight path angle $\gamma(t)$ and desired trajectory $\gamma_d(t)$, **c** velocity tracking error $e_V(t)$, **d** flight-path angle tracking error $e_\gamma(t)$

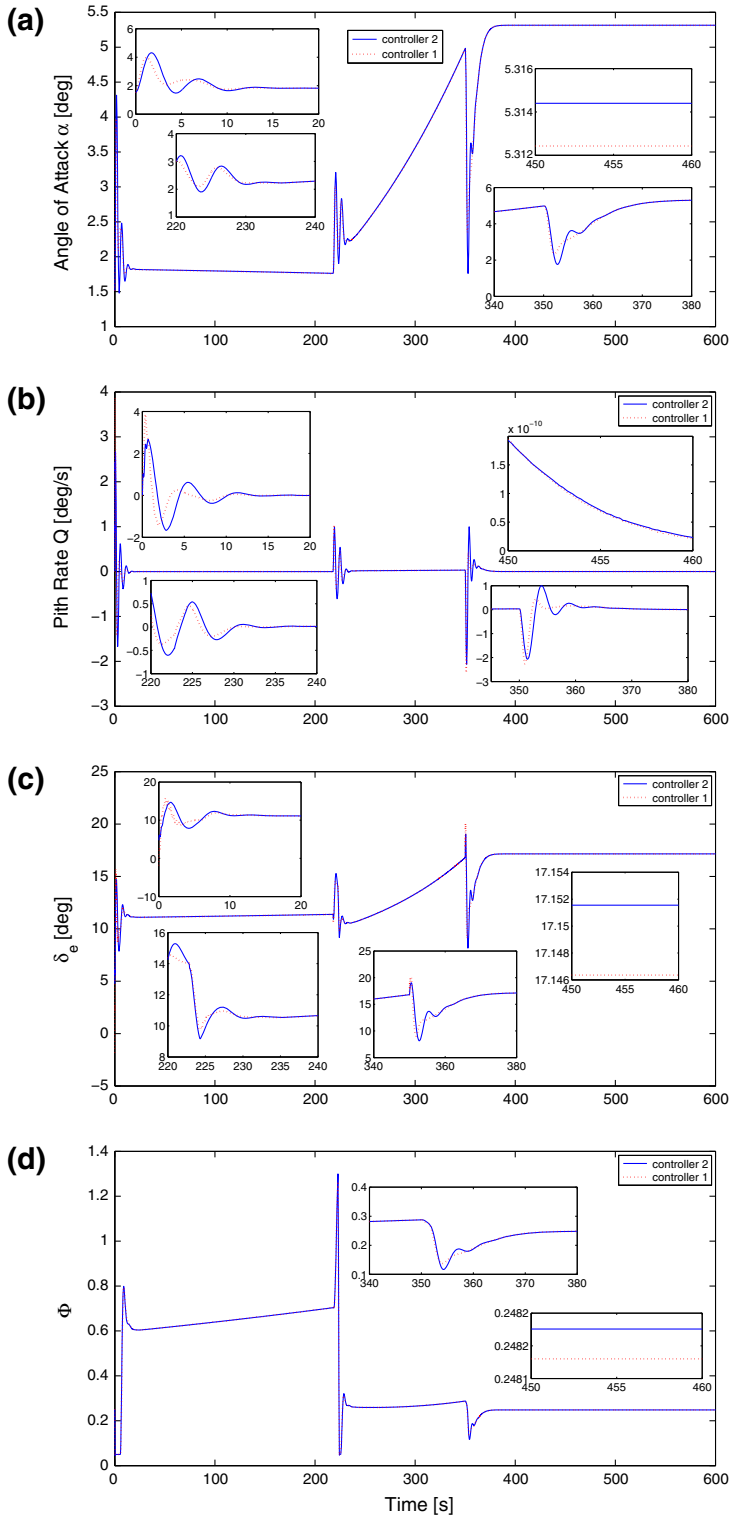

Fig. 6 Case study 2: **a** angle of attack $\alpha(t)$, **b** pitch rate $Q(t)$, **c** elevator deflection $\delta_e(t)$, **d** fuel equivalence ratio $\Phi(t)$

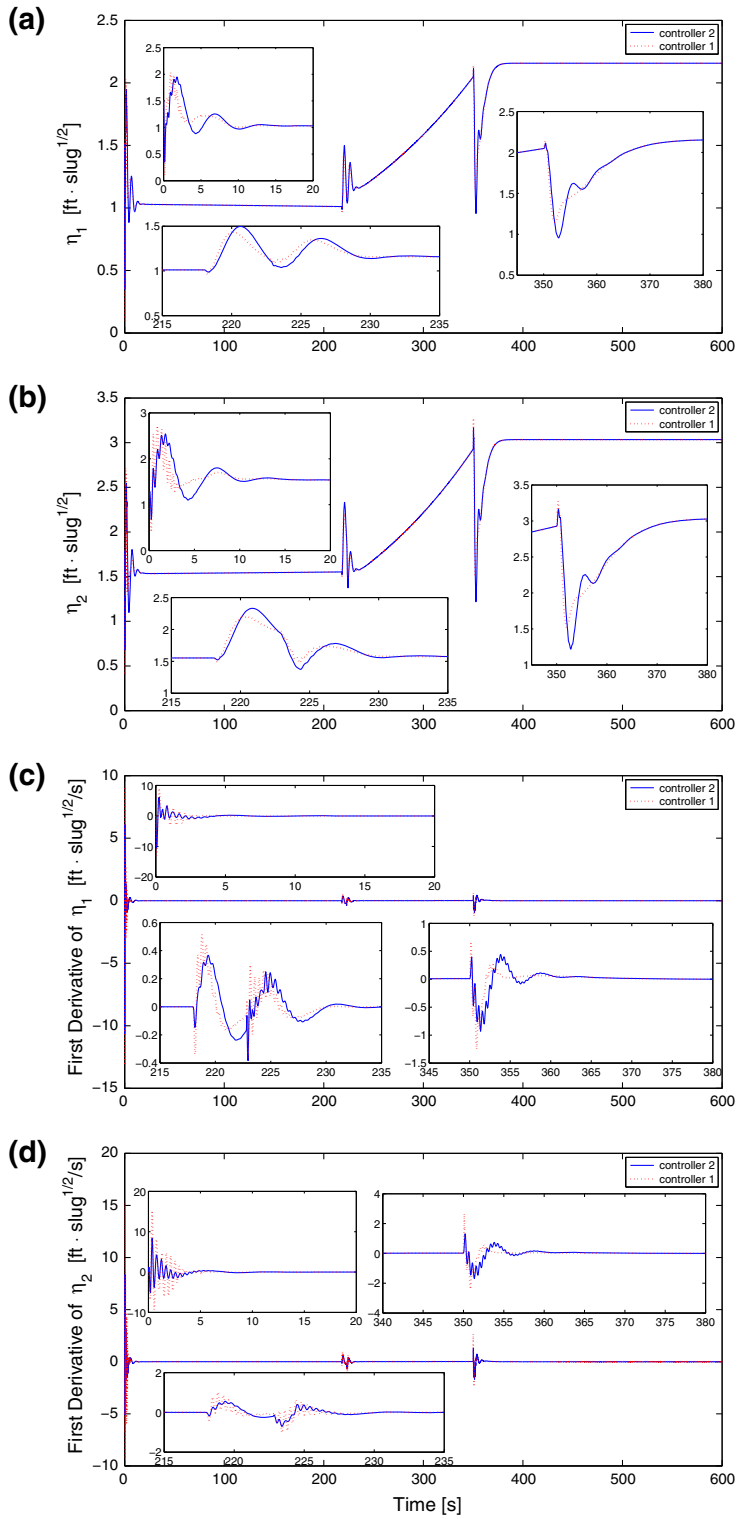

Fig. 7 Case study 2: **a** flexible mode $\eta_1(t)$, **b** flexible mode $\eta_2(t)$, **c** $\dot{\eta}_1(t)$, **d** $\dot{\eta}_2(t)$

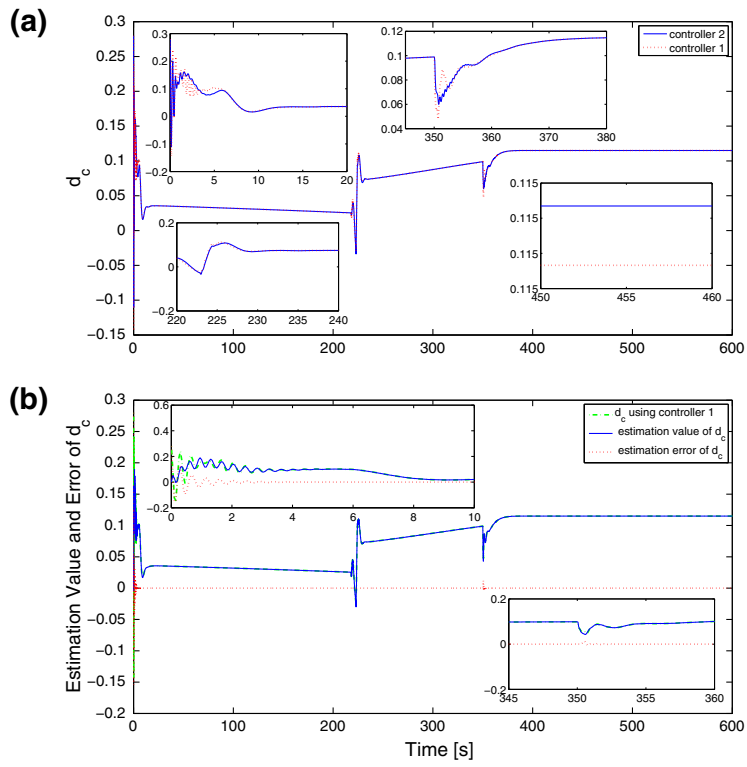

Fig. 8 Case study 2: **a** disturbance d_c, **b** estimation value and error of d_c

the previous dynamic-inversion-based nonlinear controller. One of the future research topics is to extend the result developed in this paper to FAHVs with uncertainties.

Acknowledgments This work is supported by National 973 program: 2012CB720003; National Science Foundation of China grants: 61127007, 60925012 and 91016004.

Appendix

$$\pi^V = \frac{1}{m}\begin{bmatrix} -\frac{\partial \bar{D}}{\partial V} \\ \frac{\partial T}{\partial \alpha}\cos\alpha - T\sin\alpha - \frac{\partial \bar{D}}{\partial \alpha} \\ -mg\cos\gamma \\ \frac{\partial T}{\partial \Phi}\cos\alpha \end{bmatrix}^T;$$

$$\Pi^V = \frac{1}{m}\left[\pi_1^V \;\; \pi_2^V \;\; \pi_3^V \;\; \pi_4^V\right],$$

$$\pi_1^V = \left[-\frac{\partial^2 \bar{D}}{\partial V^2} \;\; -\frac{\partial^2 \bar{D}}{\partial \alpha \partial V} \;\; 0 \;\; 0\right]^T,$$

$$\pi_2^V = \begin{bmatrix} -\frac{\partial^2 \bar{D}}{\partial \alpha \partial V} \\ \left(\frac{\partial^2 T}{\partial \alpha^2} - T\right)\cos\alpha - 2\frac{\partial T}{\partial \alpha}\sin\alpha - \frac{\partial^2 \bar{D}}{\partial \alpha^2} \\ 0 \\ \frac{\partial^2 T}{\partial \alpha \partial \Phi}\cos\alpha - \frac{\partial T}{\partial \Phi}\sin\alpha \end{bmatrix},$$

$$\pi_3^V = \begin{bmatrix} 0 \\ 0 \\ mg\sin\gamma \\ 0 \end{bmatrix}, \quad \pi_4^V = \begin{bmatrix} 0 \\ \frac{\partial^2 T}{\partial \Phi \partial \alpha}\cos\alpha - \frac{\partial T}{\partial \Phi}\sin\alpha \\ 0 \\ 0 \end{bmatrix};$$

$$\pi^\gamma = \begin{bmatrix} -\frac{\partial^2 \bar{L}/\partial V^2}{mV} - \frac{\bar{L}+T\sin\alpha}{mV^2} + \frac{g\cos\gamma}{V^2} \\ \frac{\partial \bar{L}/\partial \alpha + (\partial T/\partial \alpha)\sin\alpha + T\cos\alpha}{mV} \\ \frac{g\sin\gamma}{V} \\ \frac{(\partial T/\partial \alpha)\sin\alpha}{mV} \end{bmatrix}^T;$$

$$\Pi^\gamma = \left[\pi_1^\gamma \;\; \pi_2^\gamma \;\; \pi_3^\gamma \;\; \pi_4^\gamma\right],$$

$$\pi_1^\gamma = \begin{bmatrix} -\frac{\partial^2 \bar{L}/\partial V^2}{mV} - 2\frac{\partial \bar{L}/\partial V}{mV^2} + \frac{2(\bar{L}+T\sin\alpha)}{mV^3} - \frac{2g\cos\gamma}{V^3} \\ \frac{\partial^2 \bar{L}/\partial V \partial \alpha}{mV} - \frac{\partial \bar{L}/\partial \alpha + (\partial T/\partial \alpha)\sin\alpha + T\cos\alpha}{mV} \\ -\frac{g\sin\gamma}{V^2} \\ -\frac{(\partial T/\partial \alpha)\sin\alpha}{mV^2} \end{bmatrix},$$

$$\pi_2^\gamma = \begin{bmatrix} -\frac{\partial^2 \bar{L}/\partial V \partial \alpha}{mV} - \frac{\partial \bar{L}/\partial \alpha + (\partial T/\partial \alpha)\sin\alpha + T\cos\alpha}{mV^2} \\ \frac{\partial^2 \bar{L}/\partial \alpha^2 + (\partial^2 T/\partial \alpha^2) - T)\sin\alpha + 2(\partial T/\partial \alpha)\cos\alpha}{mV} \\ 0 \\ -\frac{(\partial^2 T/\partial \alpha \partial \Phi)\sin\alpha + (\partial T/\partial \Phi)\cos\alpha}{mV} \end{bmatrix},$$

$$\pi_3^\gamma = \left[-\frac{g\sin\gamma}{V^2} \;\; 0 \;\; \frac{g\cos\gamma}{V} \;\; 0\right]^T,$$

$$\pi_4^{\gamma} = \begin{bmatrix} -\frac{(\partial T/\partial \Phi)\sin\alpha}{mV^2} \\ -\frac{(\partial^2 T/\partial\alpha\partial\Phi)\sin\alpha + (\partial T/\partial\Phi)\cos\alpha}{mV} \\ 0 \\ 0 \end{bmatrix}.$$

References

1. Curran, E.: Scramjet engines: the first forty years. J. Propul. Power **17**(6), 1138–1148 (2001)
2. Engelund, W.: Hyper-X aerodynamics: the X-43A airframe-integrated scramjet propulsion flight-test experiments. J. Spacecr. Rockets **38**(6), 801–802 (2001)
3. Fidan, B., Mirnirani, M., Ioannou, P.: Flight dynamics and control of air-breathing hypersonic vehicles: review and new directions. In: AIAA International Space Planes and Hypersonic Systems and Technologies, Norfolk, Virginia, AIAA Paper 2003-7081 (2003)
4. Bolender, M., Oppenheimer, M., Doman, D.: Effects of unsteady and viscous aerodynamics on the dynamics of a flexible air-breathing hypersonic vehicle. In: AIAA Atmospheric Flight Mechanics Conference and Exhibit, Hilton Head, South Carolina, AIAA Paper 2007-6397 (2007)
5. Shaughnessy, J., Pinckney, S., McMinn, J., Cruz, C., Kelley, M.: Hypersonic vehicle simulation model: winged-cone configuration. NASA TM-102610 (1990)
6. Bolender, M., Doman, D.: Nonlinear longitudinal dynamical model of an air-breathing hypersonic vehicle. J. Spacecr. Rockets **44**(2), 374–387 (2007)
7. Schmidt, D.: Dynamics and control of hypersonic aeropropulsive/aeroelastic vehicles. AIAA 92-4326-CP (1992)
8. Chavez, F., Schmidt, D.: Analytical aeropropulsive/aeroelastic hypersonic-vehicle model with dynamic analysis. J. Guid. Control Dyn. **17**(6), 1308–1319 (1994)
9. Chavez, F., Schmidt, D.: Uncertainty modeling for multivariable-control robustness analysis of elastic high-speed vehicles. J. Guid. Control Dyn. **22**(1), 87–95 (1999)
10. Williams, T., Bolender, M., Doman, D.: An aerothermal flexible mode analysis of a hypersonic vehicle. In: AIAA Atmospheric Flight Mechanics Conference and Exhibit, Keystone, Colorado, AIAA Paper 2006-6647 (2006)
11. Gregory, I., Chowdhry, R., McMinn, J., Shaughnessy, J.: Hypersonic vehicle model and control law development using H_∞ and μ synthesis. NASA TM-4562 (1994)
12. Chen, M., Jiang, C., Wu, Q.: Disturbance-observer-based robust flight control for hypersonic vehicles using neural networks. Adv. Sci. Lett. **4**(5), 1771–1775 (2011)
13. Groves, K., Sigthorsson, D., Serrani, A., Yurkovich, S., Bolender, M., Doman, D.: Reference command tracking for a linearized model of an air-breathing hypersonic vehicle. In: AIAA Guidance, Navigation, and Control Conference and Exhibit, San Francisco, California, AIAA Paper 2005-6144 (2005)
14. Groves, K., Serrani, A., Yurkovich, S., Bolender, M., Doman, D.: Anti-windup control for an air-breathing hypersonic vehicle model. In: AIAA Guidance, Navigation, and Control Conference and Exhibit, Keystone, Colorado, AIAA Paper 2006-6557 (2006)
15. Sigthorsson, D., Serrani, A., Yurkovich, S., Bolender, M., Doman, D.: Tracking control for an overactuated hypersonic air-breathing vehicle with steady state constraints. In: AIAA Guidance, Navigation, and Control Conference and Exhibit, Keystone, Colorado, AIAA Paper 2006-6558 (2006)
16. Sigthorsson, D., Jankovsky, P., Serrani, A., Yurkovich, S., Bolender, M., Doman, D.: Robust linear output feedback control of an airbreathing hypersonic vehicle. J. Guid. Control Dyn. **31**(4), 1052–1066 (2008)
17. Hu, X., Wu, L., Hu, C., Gao, H.: Adaptive sliding mode tracking control for a flexible air-breathing hypersonic vehicle. J. Franklin I. **349**(2), 559–577 (2012)
18. Marrison, C., Stengel, R.: Design of robust control systems for a hypersonic aircraft. J. Guid. Control Dyn. **21**(1), 58–63 (1998)
19. Wang, Q., Stengel, R.: Robust nonlinear control of a hypersonic aircraft. J. Guid. Control Dyn. **23**(4), 577–585 (2000)
20. Xu, H., Mirmirani, M., Ioannou, P.: Adaptive sliding mode control design for a hypersonic flight vehicle. J. Guid. Control Dyn. **27**(5), 829–838 (2004)
21. Butt W., Yan L., Kendrick A.: Robust adaptive dynamic surface control of a hypersonic flight vehicle. In: 49th IEEE Conference on Decision and Control, pp. 3632–3637, Atlanta, Georgia, USA (2010)
22. Li, S., Sun, H., Sun, C.: Composite controller design for an air-breathing hypersonic vehicle. Proc. Inst. Mech. Eng. I J. Syst. Control Eng. **69**(5), 595–611 (2010)
23. Xu, B., Sun, F., Yang, C., Gao, D.: Adaptive discrete-time controller design with neural network for hypersonic flight vehicle via back-stepping. Int. J. Control **84**(9), 1543–1552 (2011)
24. Xu, B., Sun, F., Liu, H., Ren, J.: Adaptive Kriging controller design for hypersonic flight vehicle via back-stepping. IET Control Theory Appl. **6**(4), 487–497 (2012)
25. Xu, B., Wang, D., Sun, F., Shi, Z.: Direct neural discrete control of hypersonic flight vehicle. Nonlinear Dyn. **70**(1), 269–278 (2012)
26. Xu, B., Shi, Z., Yang, C., Wang, S.: Neural hypersonic flight control via time-scale decomposition with throttle setting constraint. Nonlinear Dyn. **73**(3), 1849–1861 (2013)
27. Sun, H., Li, S., Sun, C.: Finite time integral sliding mode control of hypersonic vehicles. Nonlinear Dyn. **73**(1—-2), 229–244 (2013). doi:10.1007/s11071-013-0780-4
28. Xu, B., Huang, X., Wang, D., Sun, F.: Dynamic surface control of constrained hypersonic flight models with parameter estimation and actuator compensation. Asian J. Control **16**(1), 162–174 (2014)
29. Parker, J., Serrani, A., Yurkovich, S., Bolender, M., Doman, D.: Control-oriented modeling of an air-breathing hypersonic vehicle. J. Guid. Control Dyn. **30**(3), 856–869 (2007)
30. Fiorentini, L., Serrani, A.: Adaptive restricted trajectory tracking for a non-minimum phase hypersonic vehicle model. Automatica **48**(7), 1248–126 (2012)
31. Fiorentini, L., Serrani, A., Bolender, M., Doman, D.: Nonlinear robust adaptive control of flexible air-breathing hypersonic vehicles. J. Guid. Control Dyn. **32**(2), 401–416 (2009)
32. Driels, M.: Linear Control Systems Engineering. McGraw-Hill, New York (1996)
33. Radke, A., Gao, Z.: A survey of state and disturbance observer for practitioners. In: Proceedings of the 2006

American Control Conference, pp. 5183–5188, Minneapolis, Minnesota, USA (2010)
34. Guo, L., Cao, S.: Anti-disturbance control for systems with multiple disturbances. CRC Press, Boca Raton (2013)
35. Chen, W.H.: Nonlinear disturbance observer-enhanced dynamic inversion control of missiles. J. Guid. Control Dyn. **26**(1), 161–166 (2003)
36. Liu, H., Guo, L., Zhang, Y.: An anti-disturbance PD control scheme for attitude control and stabilization of flexible spacecrafts. Nonlinear Dyn. **67**(3), 2081–2088 (2012)
37. Guo, L., Chen, W.: Disturbance attenuation and rejection for systems with nonlinearity via DOBC approach. Int. J. Robust Nonlinear Control **15**(3), 109–125 (2005)
38. Guo, L., Wen, X.: Hierarchical anti-disturbance adaptive control for non-linear systems with composite disturbances and applications to missile systems. Trans. Inst. Meas. Control **33**(8), 942–956 (2011)